crystal field model for the interpretation of the experimental results. Trying to account for the effects solely in terms of the nominal difference in the $3d$ electronic configuration in octahedral crystal field, i.e., $e_g^2 t_{2g}^3$ vs $e_g^2 t_{2g}^4$, one can attribute them to the outstanding difference between the $3d(e_g)$ and $3d(t_{2g})$ wave functions. The $3d(e_g)$ density distribution in the octahedral ligand configuration is concentrated along the bond directions, while the $3d(t_{2g})$ density is distributed in the directions in between the bonds. If the difference of -6×10^{-5} mm/sec °K in the slopes of Fig. 5 is associated with the contribution of a single $3d(t_{2g})$ electron, the contribution due to the four t_{2g} electrons in the Fe^{2+} compounds should be quadrupled. The vanishing of the effect in the $3d^6$ $(e_g^2 t_{2g}^4)$ electronic configuration may be attributed to the mutual cancellation of opposing contributions from the two different sets of electronic orbitals. In other words, the slight overall expansion of the $3d(t_{2g})$ orbitals upon raising the temperature, as reflected by the negative contribution to the thermal slope of the isomer shift, is balanced by an overall contraction of the $3d(e_g)$ orbitals.

An overall expansion of the charge-density distribution upon raising the temperature may be rationalized in terms of volume expansion. A mechanism which will produce the suggested contraction of the $3d(e_g)$ density distribution upon raising the temperature has been proposed by Shrivastava[11] on the basis of a theoretical discussion of the electron-phonon interaction. Although the author did not distinguish in his paper between the e_g and t_{2g} symmetries, it is expected that such an interaction will be substantially different for the two sets of orbitals.

The opposite behavior of the two sets of $3d$ wave functions in the octahedral bonding configuration is not that surprising. Hyperfine-interaction data indicate that covalency effects in "ionic" ferrous compounds involve opposite contributions to the two sets of orbitals.[10]

[1]H. K. Perkins and Y. Hazony, Phys. Rev. B 5, 7 (1972).
[2]S. Bukshpan and R. H. Herber, J. Chem. Phys. 46, 3375 (1967).
[3]Y. Hazony, J. Chem. Phys. 49, 159 (1968); 53, 858(E) (1970).
[4]Y. Hazony, Discuss Faraday Soc. 48, 148 (1969).
[5]D. E. Earls, Y. Hazony, and R. C. Axtmann, Bull. Am. Phys. Soc. 12, 654 (1967); Y. Hazony, R. C. Axtmann, and J. W. Hurley, Jr., Bull. Am. Phys. Soc. 13, 690 (1968); 15, 106 (1970).
[6]D. P. Johnson and J. G. Dash, Phys. Rev. 172, 938 (1968).
[7]K. K. Kelley and G. E. Moore, J. Am. Chem. Soc. 65, 1264 (1943).
[8]S. S. Todd and J. P. Coughlin, J. Am. Chem. Soc. 73, 4184 (1951).
[9]J. M. Coey, G. A. Sawatzky, and A. H. Morrish, Phys. Rev. 184, 334 (1969).
[10]Y. Hazony, Phys. Rev. B 3, 711 (1971); *Advances in Mössbauer Effect Methology*, edited by I. J. Gruverman (Plenum, New York, 1971), p. 147, Vol. 7.
[11]K. N. Shrivastava, Phys. Rev. B 1, 955 (1970).

PHYSICAL REVIEW B VOLUME 7, NUMBER 7 1 APRIL 1973

Antiferromagnetic Ordering and Crystal Field Behavior of $NiCl_2$ $4H_2O$

J. N. McElearney, D. B. Losee, S. Merchant, and R. L. Carlin
Department of Chemistry, University of Illinois at Chicago Circle, Chicago, Illinois 60680
(Received 13 July 1972)

Magnetic-susceptibility and heat-capacity measurements on single crystals of $NiCl_2 \cdot 4H_2O$, which is isomorphic to $MnCl_2 \cdot 4H_2O$ and $MnBr_2 \cdot 4H_2O$, indicate an antiferromagnetic-paramagnetic transition at (2.99 ± 0.01) °K. The large zero-field splitting of the Ni^{2+} ion in this material results in an 11 °K doublet-singlet splitting of its ground state with the doublet lying lower. A molecular-field model has been used to obtain an exchange-parameter value of $zJ/k = -5.25$ °K. The effect of the crystal field anisotropy on the transition temperature has been interpreted and the results seem to indicate that the molecular-field theory gives a better approximation than do the Green's-function techniques.

I. INTRODUCTION

Studies on a set of isomorphic materials containing different magnetic ions or different ligands, or both, are common in the area of magnetism. Unfortunately, the information which might be gained from comparisons of isomorphic materials has usually been limited, since few of those studies made to date have been made on systems which have been widely investigated at low temperatures, where the magnetic effects may be unambiguously measured. One material which is a member of an isomorphic

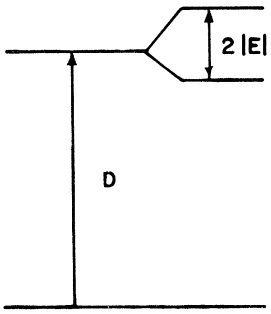

FIG. 1. The level splitting for Ni^{2+}. For negative D the figure is inverted.

series and which has been thoroughly investigated at low temperatures is $MnCl_2 \cdot 4H_2O$, which orders antiferromagnetically at 1.62°K.[1] The studies made on this material include measurements of magnetic moments,[2] magnetic susceptibilities,[3,4] heat capacities (both low[1,5] and high[6] resolution), spin flopping,[7,8] relaxation processes,[3,4] proton and chlorine NMR,[9] and magnetothermodynamic characteristics.[10–14] In order to investigate the effect of a change in spin and addition of a large zero-field splitting on the magnetic ordering observed in $MnCl_2 \cdot 4H_2O$, magnetic-susceptibility and heat-capacity measurements, reported here, have been made at low temperatures on $NiCl_2 \cdot 4H_2O$, which has been reported as being an isomorph of $MnCl_2 \cdot 4H_2O$.[15] The effect of an axial crystal field on the Ni^{2+} ion is to split the threefold-degenerate ground state into a doublet and a singlet separated by an energy D. If there is a rhombic component to the crystal field, the doublet is in turn split by $2E$. Thus the results have been interpreted on the basis of the level scheme shown in Fig. 1 and the spin Hamiltonian appropriate to a spin-1 system,

$$\mathcal{H} = D(S_z^2 - \tfrac{2}{3}) + E(S_x^2 - S_y^2) + \mu_B \sum_i g_i H_i S_i \ . \qquad (1)$$

In addition, the molecular-field theory has been used to obtain a value for the exchange parameter J, and the theoretical relationship of D, J, and the ordering temperature is considered.

II. EXPERIMENTAL

A. Crystal Characteristics

Single crystals of $NiCl_2 \cdot 4H_2O$ were grown over a six-week period from an aqueous solution of reagent grade $NiCl_2 \cdot 6H_2O$. This solution was kept in a temperature-controlled bath at a temperature of 50.0 ± 0.2°C. The temperature stability of the bath was better than 0.01°C. The crystals, which grow with a habit similar to that given by Groth[16] for $MnCl_2 \cdot 4H_2O$, analyzed correctly. Several interfacial angles of the nickel compound were measured with a contact goniometer and were found to correspond to those reported for $MnCl_2 \cdot 4H_2O$, thus indicating the isomorphism of the two materials. Precession photographs of the nickel compound were taken to check further the isomorphism. The results indicate $NiCl_2 \cdot 4H_2O$ is monoclinic with cell parameters $a = 10.90$ Å, $b = 9.35$ Å, $c = 6.00$ Å, and $\beta = 100.5°$. These values compare well with those[17] of $MnCl_2 \cdot 4H_2O$, which is also monoclinic, of space group $P2_1/n$, with $a = 11.186$ Å, $b = 9.513$ Å, $c = 6.186$ Å, and $\beta = 99.74°$. There is less than a 3% difference between the sets of parameters and thus there can be little doubt of the isomorphism of the two compounds. It should be noted that the compound $MnBr_2 \cdot 4H_2O$ reportedly is isomorphic to these materials also.[18]

The important features to note about the structure of $MnCl_2 \cdot 4H_2O$, which has four molecules in the unit cell, are the following: There are only two magnetically inequivalent molecules in the unit cell; the chlorine atoms in the octahedral molecular unit are in cis positions; the molecular unit is severely distorted from a perfect octahedron with some of the angles between the ligands and the manganese ion deviating as much as 8°–11° from the values for a perfect octahedron. Thus, at least physically, the molecule lacks even a twofold axis of symmetry. Although the molecular unit in the nickel compound may be more or less distorted than that in $MnCl_2 \cdot 4H_2O$, the lattice parameters suggest that the differences should be small. A final point of interest is that the hydrogen bonding was determined in the structural analysis of $MnCl_2 \cdot 4H_2O$ and that only four of the eight hydrogen atoms of a molecular unit participate. Undoubtedly this bonding plays an important role in the magnetic properties of the compounds and although the relation should be investigated more thoroughly, no attempt will be made here.

B. Temperature Measurements

Temperatures in both the susceptibility and heat-capacity experiments were measured with encapsulated germanium resistance thermometers. The one used in the heat-capacity measurements was a standard model[19] supplied with a calibration curve from 1.5 to 100°K. The calibration of this thermometer was extended to lower temperatures using vapor-pressure measurements made on liquid helium with a McLeod gauge. These measurements were converted to temperatures using the T-58 conversion table.[20] The thermometer used in the susceptibility measurements was specially constructed by the manufacturer[19] to contain no solder (to avoid superconducting transition effects) and was calibrated against the heat-capacity thermometer in the stainless-steel Dewar to be described in what follows.

The temperature-resistance calibration points were used to determine the coefficients C_i in the calibration curve used for interpolation of tempera-

tures,

$$\ln(R) = \sum_{i=0}^{21} C_i [\ln(T)]^i , \qquad (2)$$

where R is the thermometer resistance at the absolute temperature T. A least-squares fit of the calibration data to this equation was done in double precision (as were all calculations) on the UICC IBM 360/50 computer and resulted in a fit which was within the manufacturer's reported uncertainties in temperatures. To avoid any unnatural oscillations in the curve, the first and second derivatives of this curve were examined for any unusual behavior, but none were noted below 50 °K. (Above 50 °K a lower-degree polynomial must be used.) Given a resistance value and the coefficients of the fit, the method of bisection was used to determine the temperature which then satisfied Eq. (2).

The resistance of a thermometer during a run was determined potentiometrically using a Leeds and Northrup K-5 potentiometer facility and a constant-current supply. Currents of 1, 10, or 100 μA were used, depending upon the temperature region, in order to avoid thermometer self-heating effects. Resistance values were read out directly in the susceptibility measurements using the K-5's electronic null detector. An off-null technique was used in conjunction with a strip-chart recorder to determine thermometer-resistance values in the heat-capacity measurements.

C. Heat-Capacity Measurements

Heat-capacity measurements were made in a calorimeter similar to one previously described.[21] Some details of the present apparatus will be given here, since several modifications to the original design have greatly improved its capability, allowing temperatures as low as 0.85 °K to be attained and held for up to 24 h. Basically, the calorimeter (shown in Fig. 2) is of the type in which temperatures below 4.2 °K are achieved by pumping on a small container of liquid ^{4}He which is isolated by vacuum from the main reservoir of liquid ^{4}He. The oxygen-free-high-conductivity (OFHC) copper container is supported by three thin-wall type 321 stainless-steel pumping tubes which pass through a brass block immersed in liquid ^{4}He. Right-angle bends in the pumping lines inside the brass block act as traps to catch radiation coming down the pumping lines from their room-temperature ends. Two of the supporting tubes ($\frac{1}{8}$-in. o.d.) pass through the helium container into the sample region below it. (Ten 40-gauge Formvar-insulated-manganin electrical leads pass through one of these tubes.) The third tube ($\frac{1}{4}$-in. o.d.) is the helium-container pumping line which is constricted at its bottom by a 0.030-in. hole in the top of the helium container. This constriction reduces the superfluid-helium flow up the pumping line, the main limiting factor in reaching temperatures below 1.2 °K with ordinary techniques. The filling line for the helium container is a stainless-steel capillary tube (0.04-in. o.d., 0.03-in i.d.) which is wound around the pumping tube and is connected to a needle valve in the main helium reservoir. To ensure a minimum amount of heat input to the helium container, the three supporting tubes and the capillary line are thermally tied together at two levels by copper disks which also act as radiation shields.

The crystal upon which measurements are to be made is suspended with nylon thread below the helium container and the germanium thermometer is tied to it and thermally anchored with Apiezon N grease. A 1-ft length of 0.0014-in. diam Evanohm[22] wire previously attached to the crystal with

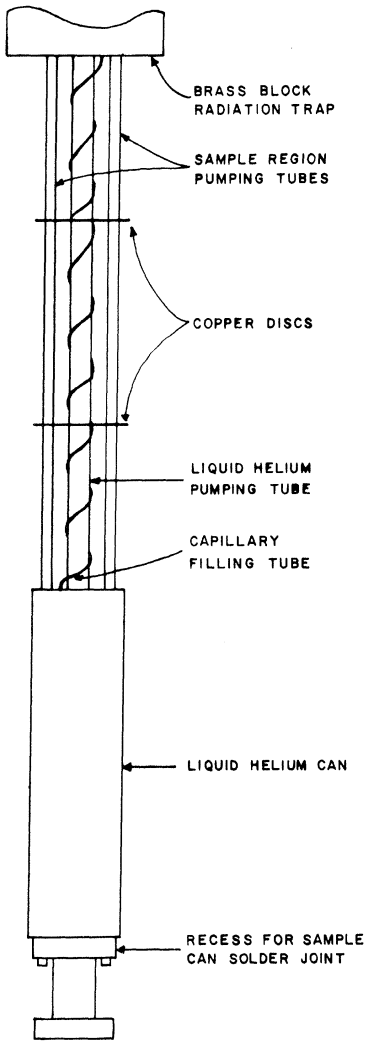

FIG. 2. The main part of the calorimeter described in the text.

a small amount of GE 1202 varnish acts as a heater. After the electrical leads have been attached, the sample region is surrounded by an OFHC copper can which is soldered onto the bottom of the helium container with Cerrolow 117 solder. Prior to cooldown to 4.2 °K, both the regions inside and outside the sample can are filled with helium gas at a pressure of 1 Torr at 77 °K. When the assembly has been cooled to 4.2 °K, the region surrounding the sample can and helium container is evacuated and liquid helium is admitted to the container through the capillary fill line. With the capillary-line needle valve closed, the temperature of the helium in the container is then reduced by pumping on it. When the lowest temperature is reached, the helium exchange gas in the sample can is removed by pumping for up to an hour before making measurements.

Data are then taken using standard heat-pulse techniques. An electronic timer times and controls the input of current from a constant-current source and the voltage across the sample heater is measured with a high-impedance microvoltmeter. The rate of change of the sample's temperature before and after each heat pulse is followed with time on an x-t chart recorder and appropriate corrections are made for the drifts in determining the temperature change due to the heat pulse.

The accuracy of the heat-capacity data is determined by the accuracy with which the change in temperature for each data point can be determined. Depending upon the drift rates and their constancy, this is between 1 and 5%. (The high accuracy and precision of the electronics enables the heat input to be determined with less than 0.5% uncertainty.) The measured heat capacity must be slightly high owing to the addenda on the crystal, but runs on significantly different-sized crystals of the same material with essentially the same amount of addenda have indicated this contribution to be negligibly small for heat capacities in the range reported here.

D. Susceptibility Measurements

Susceptibility experiments were carried out in a Janis[23] 6DT stainless-steel Dewar, which allows isothermal experiments to be done between 1.5 and 300 °K. Samples are placed in a sample chamber which is kept vacuum isolated from the main reservoir and is supplied with gaseous or liquid helium from the reservoir by means of a capillary tube and a needle valve. The rate of pumping on this sample chamber, the influx rate of the cryogen, and its temperature, all control the temperature at the sample site. The main method used is the latter, in which the influx cryogen's temperature is controlled by use of an electronic temperature controller which varies the temperature of a copper block through which the helium must pass before reaching the sample chamber. Temperatures stable to better than 0.01 °K can generally be achieved.

Measurements of a sample's susceptibility were made using a 17-Hz mutual-inductance bridge[24] in conjunction with a coil placed in the Dewar around the outside of the sample chamber, a technique similar to one previously described.[25] The coil used consisted of a 2500-turns/in. primary wound on a phenolic coil form of 0.875-in. o.d. A three section 10 600-turns/in. secondary was wound over the primary. Both primary and secondary were wound with 40-gauge Formvar-insulated copper wire. The primary was 6.5 in. long and, since the outer sections of the secondary were wound opposite to the central one, it was possible to place the sample at the center of the entire coil, assuring maximum homogeneity in the field (estimated to be 15 Oe) at the sample site. The coil was placed in the main helium reservoir of the Dewar around the outside of the sample chamber, as shown schematically in Fig. 3. With the coil thus at the fixed temperature of 4.2 °K, its characteristics remained the same during a run. The change in the mutual inductance of the coil (as read from the bridge) due to a change in the susceptibility of a sample was converted to susceptibility units by use of a conversion factor previously determined within 1% from measurements on a spherically ground sample of $(NH_4)_2Mn(SO_4)_2 \cdot 6H_2O$, a substance which obeys[26] Cu-

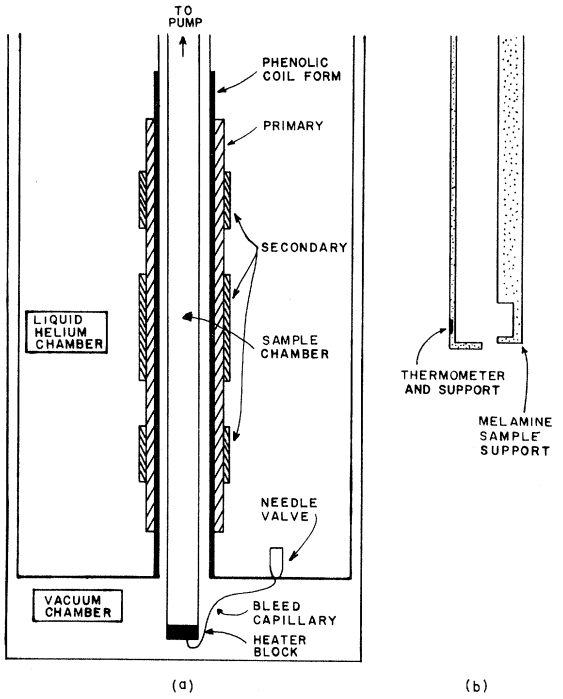

FIG. 3. The Dewar-inductance-coil arrangement used in the susceptibility measurements.

rie's law above 1 °K. Although the net mutual inductance of the empty coil fluctuates somewhat from run to run, experiments have indicated that the bridge conversion factor remains constant from run to run. The mutual inductance of the empty coil is determined for each run by removing the sample (which is on a cotton-melamine support rod) from the coil. Although this value is obtained at only one temperature, experiments have indicated that it is constant between 1.5 and 25 °K. However, fluctuations in the bridge electronics cause a small fluctuation in this value during a run. This fluctuation is the main source of uncertainty in the susceptibilities measured and amounts to ±0.002 emu/mole for the larger crystal used in this study.

III. RESULTS AND DISCUSSION

A. Heat-Capacity Results

Heat-capacity measurements were made from 0.85 to 25 °K on two single crystals of weights 3.709 and 4.672 g. The results are shown in Figs. 4 and 5. There are three important features to note about the data. First, the sharp peak at 2.99 ±0.01 °K suggests a second-order phase transition to a magnetically ordered state at lower temperatures. Secondly, the failure of the heat capacity to drop to zero more sharply above the transition, as normally seen in the $MnCl_2 \cdot 4H_2O$ data,[1] indicates the presence of a Schottky anomaly due to the zero-field splitting of the ground state of the Ni^{2+} ion. Finally, the slight bump in the data near 5 °K implies the presence of $NiCl_2 \cdot 6H_2O$ impurities in both samples. (The impurities are observed because the magnetic ordering at 5.34 °K in $NiCl_2 \cdot 6H_2O$ gives rise to a large heat capacity in that region.[27]) A careful analysis of the data indicates the amount of impurities in the two crystals to be about 3 and 5%, respectively. Since the crystals seemed perfect, the most likely source of these impurities must be occluded solution which produced the hexahydrate species either upon cooling down from the 50 °C growth temperature of the crystals or upon further cooling down to measurement temperatures. A slower growth rate probably would have avoided this problem.

The presence of the magnetic transition and the fact that the Schottky contribution is not actually resolved both indicate that the ground state of the Ni^{2+} ion in this crystal is the doublet, since otherwise there would be no magnetic ordering and the height of the Schottky anomaly would be greater, the anomaly probably being resolved in the process. The partition function in zero field for the level scheme shown in Fig. 1 is

$$Z_0 = 1 + e^{-(D-E)/kT} + e^{-(D+E)/kT} . \quad (3)$$

The specific heat due to the level splitting may then be numerically calculated using

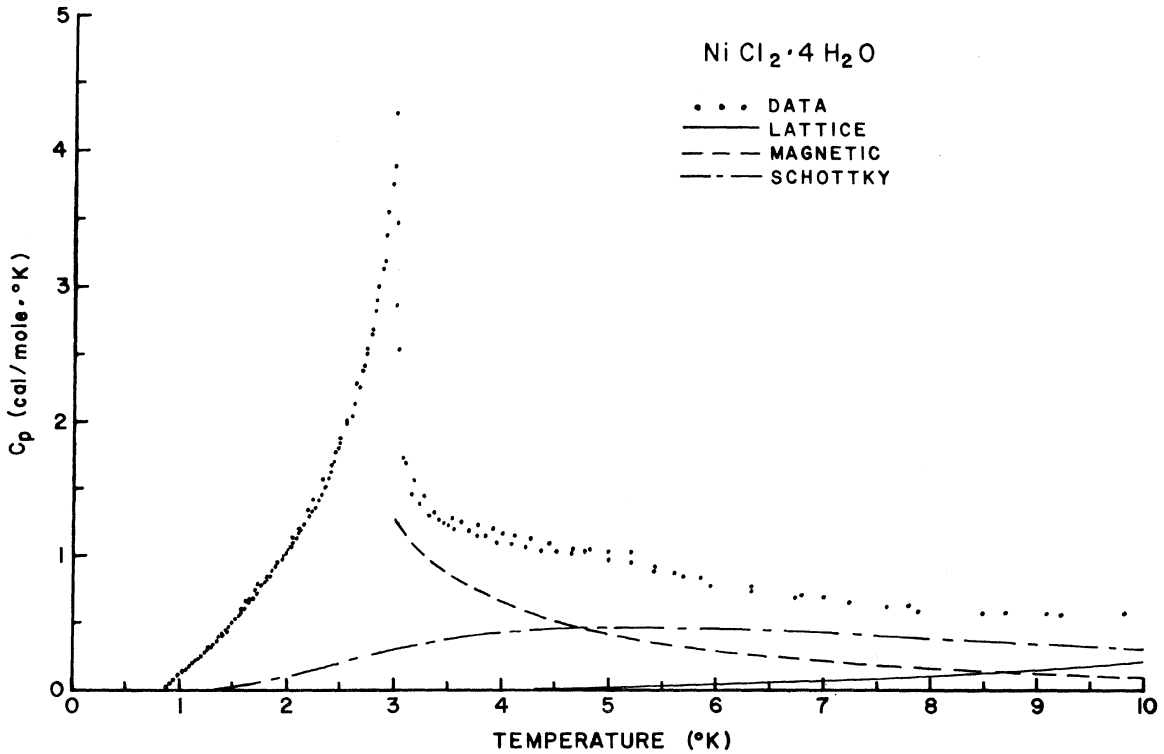

FIG. 4. The specific heat of $NiCl_2 \cdot 4H_2O$ from 0 to 10 °K. The contributions from the three sources are also shown.

$$C_{\text{Schottky}} = Nk\frac{E(T_1) - E(T_2)}{T_1 - T_2} \quad , \tag{4}$$

where N is the number of moles of Ni^{2+}, $|T_1 - T_2| \ll 1$ and $E(T)$ is the average energy at a given temperature T. In addition to an expected lattice contribution to the specific heat proportional to T^3, a contribution proportional to T^{-2} is also expected in the paramagnetic state above the transition. It has been assumed that the above contributions may be separated and that the equation

$$C_{\text{tot}} = C_{\text{Schottky}}(D, E) + AT^3 + BT^{-2} \tag{5}$$

may thus be used to fit the data in the paramagnetic region. The parameters resulting from this fit are

$D/k = -11.5 \pm 0.1\,^\circ\text{K}$,

$E/k = 0.1 \pm 0.1\,^\circ\text{K}$,

$A = (2.18 \pm 0.01) \times 10^{-4}$ cal/mole °K,

$B = 10.8 \pm 0.1$ cal °K/mole .

The separate contributions these parameters make to the heat capacity are shown between 0 and 10 °K in Fig. 4. The total fitted curve is shown over the entire measured region in Fig. 5, and although there are consistent deviations of the data about the curve, it is seen to be quite satisfactory for such a large temperature interval.

The entropy change associated with the magnetic part of the heat capacity (the measured specific heat less the lattice contribution) has been calculated (extrapolations to infinite temperatures have been accomplished through use of the fitted parameters) and agrees with the value expected for a spin-1 system, $R\ln 3$. Thus it should be expected that no important contributions to the magnetic specific heat lie outside the region of measurement. Additionally, it should be noted that approximately half of the entropy change lies above the ordering temperature, in part reflecting the presence of the Schottky anomaly in that region.

It is important to compare how close the value of A is to that obtained for the isomorph $MnBr_2 \cdot 4H_2O$, 2.24×10^{-4} cal/mole °K.[18] The value obtained for $MnCl_2 \cdot 4H_2O$ is slightly different (3.50×10^{-4} cal/mole °K),[1] but an analysis of the published data indicates that the value obtained here for $NiCl_2 \cdot 4H_2O$ could reasonably fit those data. These facts are further evidence for the isomorphism of the compounds. Another interesting point is that the constant B very nearly fits into the pattern previously noted regarding that parameter in the compounds $MnCl_2 \cdot 4H_2O$, $MnBr_2 \cdot 4H_2O$, and $CuCl_2 \cdot 2H_2O$: the proportionality of that parameter to the square of the ordering temperature with a proportionality constant near 1 cal/mole °K.[28] Thus, it would seem that the same formula used to interpret the $CuCl_2 \cdot 2H_2O$ data,

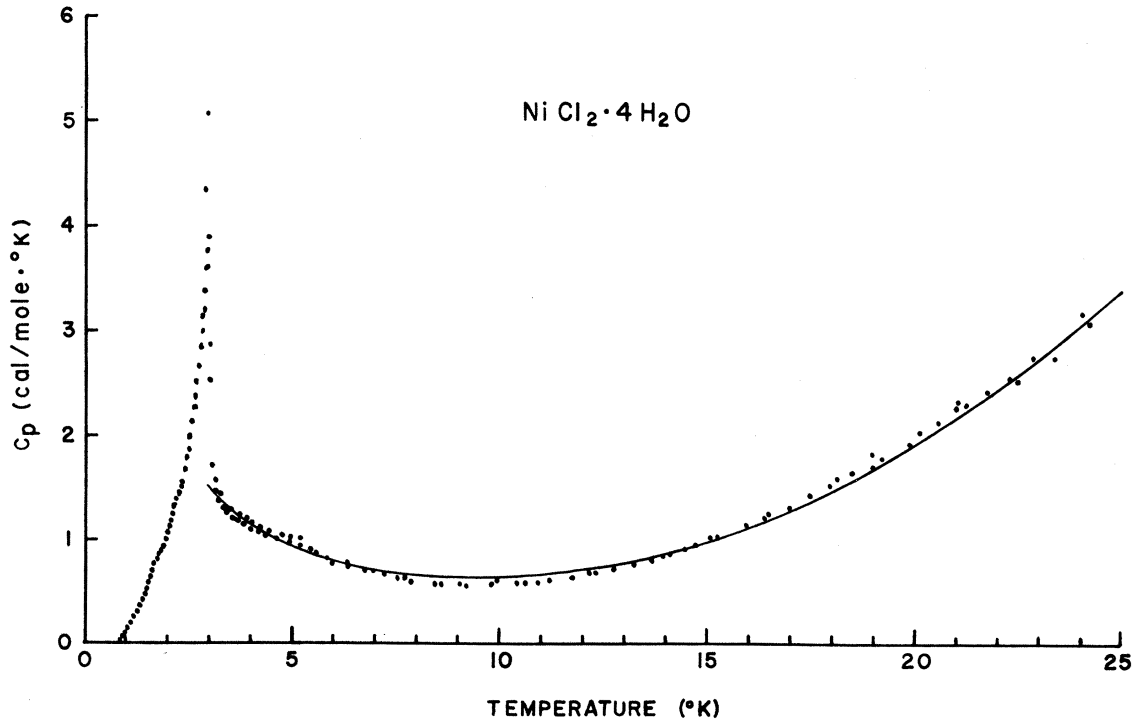

FIG. 5. The specific heat of $NiCl_2 \cdot 4H_2O$ from 0 to 25 °K. The solid line represents the specific heat calculated from the fitted parameters.

$$B = 3RT_N^2/2z \ , \qquad (6)$$

where T_N is the ordering temperature, R is the gas constant, and z is the number of nearest neighbors of each magnetic ion, might be used here also.

Substitution of the experimentally determined quantities results in a value for z of 2.48. Note that in the case of $CuCl_2 \cdot 2H_2O$, z was determined to be 3, which is in fair agreement with the actual value of 2 which results from the linear-chain nature of that material. Although the data for $MnCl_2 \cdot 4H_2O$ were not previously analyzed with this formula, values for z may be calculated from the published[5] information and are given in Table I. These values conflict with the value of 6 reported as describing well the data in both cases[5] but are consistent with the observation that there are definitely four nearest magnetic neighbors to any given magnetic ion. (The eight nearest magnetic neighbors to any given manganese ion are grouped into pairs at distances from that ion of 5.63, 5.74, 6.10, and 6.19 Å. Note that these values, based on the published structure, are different from those of Ref. 5 which were based on a different study.)

TABLE I. The nearest-neighbor predictions of Eq. (6) for the three isomorphs and their ordering temperatures.

	$MnCl_2 \cdot 4H_2O$	$MnBr_2 \cdot 4H_2O$	$NiCl_2 \cdot 4H_2O$
Near neighbors ($=z$)	4.1	2.8	2.5
Experimental T_N (°K)	1.61	2.14	2.99

B. Magnetic Susceptibility Results

Susceptibility measurements along the three perpendicular crystallographic directions a', b, and c were made between 1.5 and 20 °K on two different single crystals of weights 0.194 and 0.081 g. The smaller crystal was used for measurements along the a' axis only. The results of these measurements are shown in Fig. 6. The uncertainty in the measurements amounts to about twice the height of the triangular symbols. Several important features are to be noted. First is the anisotropy which exists over the entire temperature region which is indicative of the large zero-field splitting observed in the specific-heat measurements. Second is the general relative behavior of the three curves: the leveling off of the susceptibility in two directions and its dropping in the third as the temperature drops below about 4 °K. This behavior, of course, is typical of antiferromagnetic ordering and implies that the spin alignment is along the c axis. A third observation is that the c-axis susceptibility does not seem to be approaching zero at $T = 0$ as it should. There are two plausible reasons for this: the presence of a small amount of randomly oriented $NiCl_2 \cdot 6H_2O$ impurity

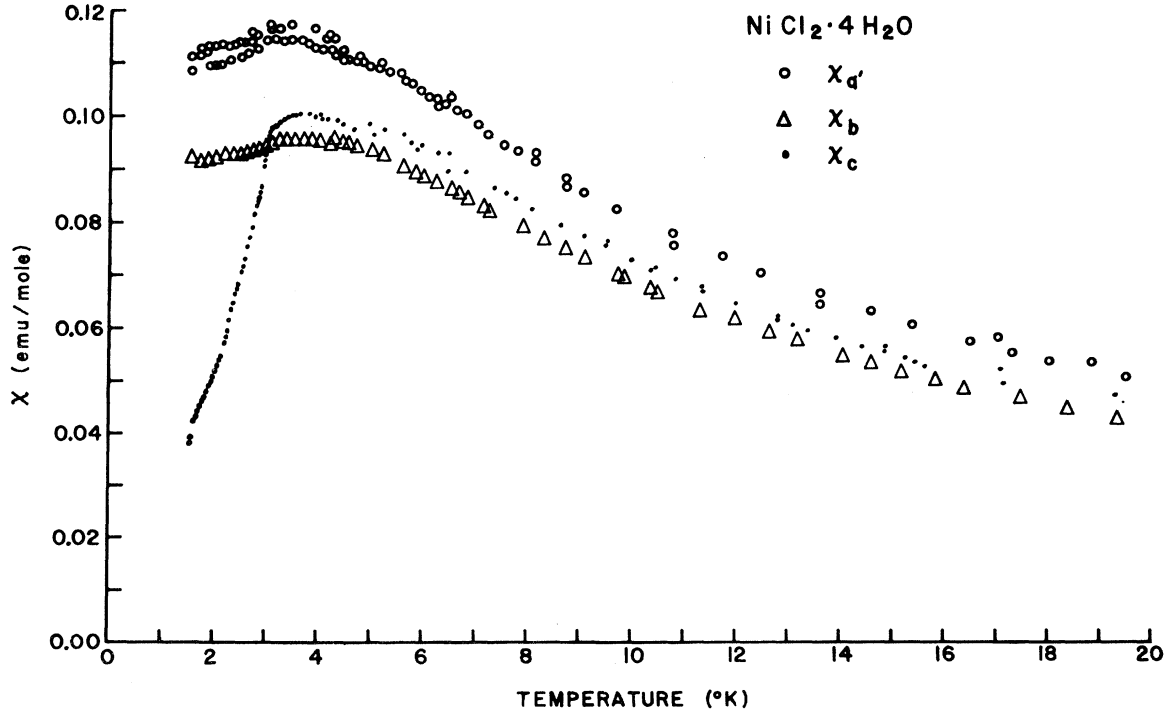

FIG. 6. The magnetic susceptibility of $NiCl_2 \cdot 4H_2O$ from 0 to 20 °K along the a', b, and c axes.

similar to that present in the specific-heat samples, or the lack of perfect alignment of the crystal along the preferred axis, which, in addition, might be slightly different from the c axis. Either situation would cause the c-axis susceptibility to be slightly higher than expected, with this effect only being observable in the ordered state at temperatures where the actual susceptibility is relatively small. Owing to the size of the crystal used, imperfect alignment along the c axis seems the most likely explanation. In addition, the same reasoning also may be applied to the slight difference seen at low temperatures in the pair of a'-axis measurements. A fourth important fact is that a careful study of the data shows the presence of inflection points in all three curves below 4 °K. Although the quality of the present data is not sufficiently good to warrant a careful calculation of the temperatures at which these inflection points occur, it is obvious that they all occur very close to the transition temperature observed in the heat-capacity measurements. This behavior is in agreement with theoretical predictions.[29,30] Finally, an interesting feature is that the inflection points of the b- and c-axis data seem to occur at the same susceptibility value so that there is little or no anisotropy in the bc plane at the ordering temperature.

The susceptibility data have been fitted in the following manner: First, the molecular susceptibilities were calculated using the single-ion Hamiltonian of Eq. (1), with the fitted parameters being D, E, g_x, g_y, and g_z; then the macroscopic susceptibilities along the a', b, and c axes were calculated for a monoclinic crystal using those molecular susceptibilities, with the fitted parameters being the Euler angles describing the orientation of the molecular axes of a molecule in the crystal relative to the a', b, and c axes; finally, the macroscopic susceptibilities thus calculated were corrected for the presence of exchange by means of a molecular-field approximation, with zJ, the product of the number of interacting magnetic neighbors with the exchange interaction, being the fitted parameter.

The energy levels for field measurements along the molecular x, y, and z axes are readily calculated from Eq. (1).[31] The partition function Z_H in each case may then be calculated and the molecular magnetic susceptibility obtained from

$$K_i = \frac{kT}{H}\frac{\partial}{\partial H}\ln(Z_H), \qquad i = x,\ y,\ z. \tag{7}$$

The results, in the approximation of small fields, have been previously given[32] and are

$$K_i = 2g_i^2\mu_B^2\delta_i, \tag{8}$$

where

$$\delta_x = \frac{1}{D+E}\,\frac{1-e^{-(D-E)/kT}}{Z_0},$$

$$\delta_y = \frac{1}{D-E}\,\frac{e^{-(D-E)/kT}-1}{Z_0},$$

$$\delta_z = \frac{1}{2E}\,\frac{e^{-(D-E)/kT}-e^{-(D+E)/kT}}{Z_0},$$

and where k is the Boltzmann constant, T is the absolute temperature, and Z_0 is given by Eq. (3). Since previous measurements of the g values for Ni^{2+} have shown essentially isotropic values,[33] the present data were fitted assuming $g_x = g_y = g_z$. The equations describing macroscopic susceptibility measurements in the a', b, and c directions are readily written down upon consideration of the relative orientations of the x, y, and z axes to the a', b, and c set. The macroscopic monoclinic symmetry, which also must be taken into account, results in an off-diagonal term in the susceptibility tensor which couples the a' and c directions.[34] The equations used here for molar susceptibility are

$$\chi_j = N\sum K_i C_{ij}^2, \quad j = (a',\ b,\ c), \quad i = x,\ y,\ z \tag{9}$$

where C_{ij} is the direction cosine between the i axis and the j axis and which, since there are no obvious axes of symmetry in the molecular unit which might be used to set the z axis, must be determined for each (i, j) pair by fitting the data. These equations, then, describe the data that would be obtained if there were no exchange. To include an exchange effect, a molecular exchange field is "turned on." This field is given[32] by

$$H_i' = \frac{2zJ}{Ng_i^2\mu_B^2}\chi_i' H_i, \quad i = a',\ b,\ \text{or } c \tag{10}$$

where χ_i' is the exchange-corrected susceptibility actually measured and where the external field H_i and the resulting exchange field are in the i direction. Since the molecular g values are isotropic each g_i is also equal to that same value. Then, with this additional field turned on when there is a measuring field, the measured magnetization in the i direction is given by

$$M_i = \chi_i(H_i + H_i'), \quad i = a',\ b,\ \text{or } c. \tag{11}$$

But then, since by definition the measured susceptibility is given by

$$\chi_i' = \lim_{H_i \to 0}\frac{M_i}{H_i}, \qquad i = a',\ b,\ \text{or } c \tag{12}$$

the exchange-corrected susceptibility is given by [combining Eqs. (10–12)]

$$\chi_i' = \frac{\chi_i}{1-(2zJ/Ng_i^2\mu_B^2)\chi_i}, \quad i = a',\ b,\ \text{or } c. \tag{13}$$

Fits of the data using these equations resulted in the same values for D and E determined from the specific-heat data. In addition, the following quantities were found:

$zJ/k = -5.25 \pm 0.10\,^{\circ}\mathrm{K}$,

$g_x = g_y = g_z = 2.28 \pm 0.01$.

Also, the relative orientation of the x, y, and z axes with the a', b, and c set was found from the fit. The resulting direction cosines are given in Table II, where the uncertainty in the sign of b results from the monoclinic symmetry.

The susceptibility curves resulting from the above parameters are shown in Fig. 7 along with the data set to which each one was fitted. The quality of the fits is quite gratifying, especially considering that a molecular-field approximation has been used. Of course the fitted curves begin to deviate from the data in the region of the transition, but from that point to near 20 °K, all three curves fit the data within the stated experimental uncertainties. (The two highest-temperature b-axis points are slightly outside the error bounds.) It should be pointed out that there seem to be consistent deviations of the data about the fitted curves; this behavior may be a result of using the molecular-field approximation over such a wide temperature interval. The important facts are that the data are well fitted and that the fits show anisotropy in the paramagnetic state similar to that shown by the data.

TABLE II. Direction cosines C_{ij} between the crystallographic axes (a', b', c) and the molecular axes (x, y, z) for $NiCl_2 \cdot 4H_2O$.

	a'	$\pm b$	c
x	0.702	0.170	0.693
y	−0.692	0.391	0.606
z	0.169	0.904	−0.392

C. Discussion

Several interesting observations regarding the magnetic behavior of $NiCl_2 \cdot 4H_2O$ in relation to that of its isomorphs can be made. First, the extremely large single-ion anisotropy which has been observed should be noted. Although Ni^{2+} is expected to have a large value for D, the value observed in this study appears to be the largest reported to date. With the one exception of a value for D of 43 cm^{-1}, which was reported[35] with some skepticism for $Ni(NH_3)_6Cl_2$, the largest reported values of D/k for nickel compounds range from 6–8 °K.[35–41] Undoubtedly, the presence of such a distinct axial nature for the cis-$NiCl_2(OH_2)_4$ molecular unit, as shown by the small value of E, could not have been expected. Indeed, the molecular-quantization axes found in

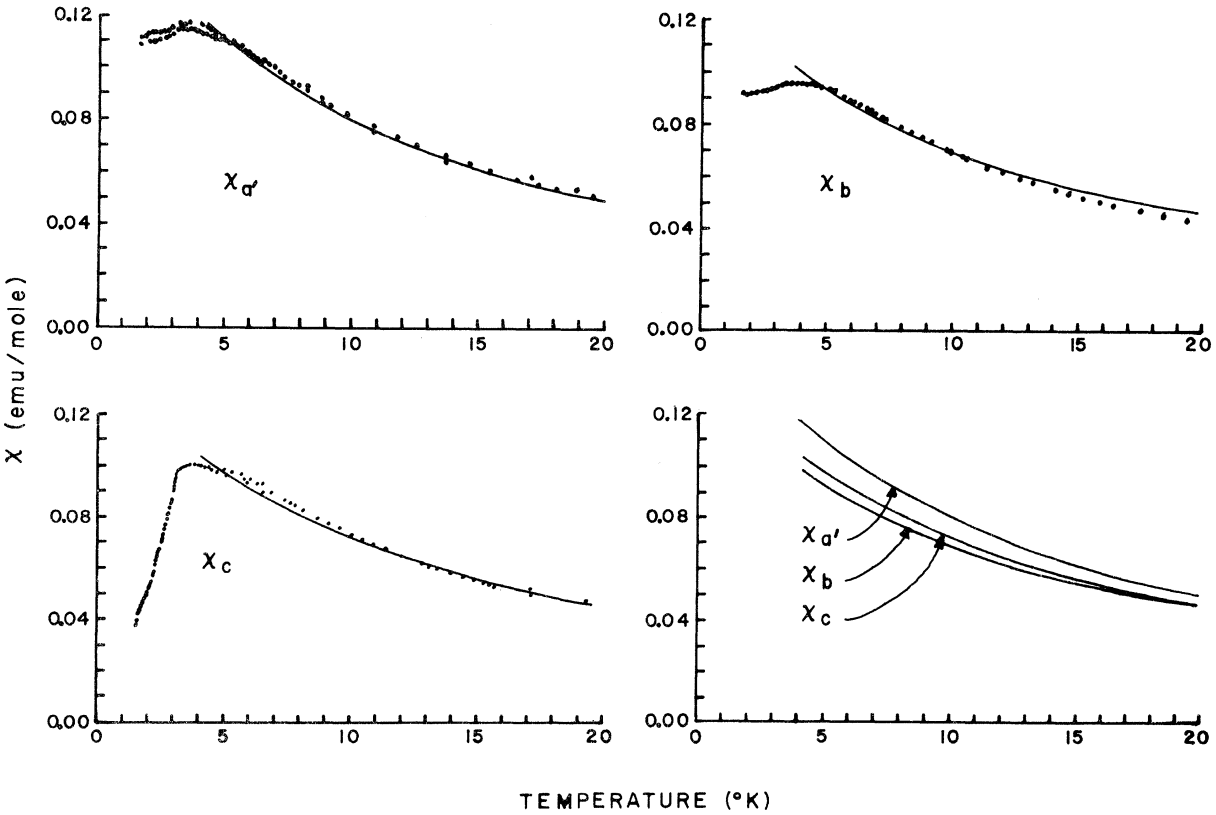

FIG. 7. Comparison of the fitted susceptibility curves to the corresponding data and the resulting anisotropy.

TABLE III. Experimental values of $|zJ/k|$, the corresponding molecular-field predictions for the ordering temperatures, and the experimentally observed ordering temperatures for the three isomorphs.

	$MnCl_2 \cdot 4H_2O$	$MnBr_2 \cdot 4H_2O$	$NiCl_2 \cdot 4H_2O$
Spin	$\frac{5}{2}$	$\frac{5}{2}$	1
$\lvert zJ/k \rvert$ (°K)	0.34	0.47	5.25
Molecular-field T_N (°K)	2.00	2.77	7.00
Experimental T_N (°K)	1.62	2.14	2.99

this study bear no obvious relation to the components of the molecular unit. Although a theoretical point-charge–point-dipole calculation of the molecular axes might prove interesting, it has not been attempted. Another interesting point is that the easy axis of magnetization (the c axis) is the same in all three of the isomorphic compounds. Although this might have been anticipated, there is a similar pair of isomorphs, $NiCl_2 \cdot 6H_2O$ and $CoCl_2 \cdot 6H_2O$, in which this is not the case.[42,43] The presence of this magnetic, as well as crystallographic, isomorphism should allow some potentially interesting experiments on the mixed material $(Mn, Ni)Cl_2 \cdot 4H_2O$.

Perhaps the most interesting point regarding the three isomorphs is the relatively large value for the transition temperature in the nickel compound. A clue to the cause may be obtained from the information in Table III in which values of $|zJ/k|$ have been obtained using molecular-field models applied to the values reported[5] for the perpendicular susceptibilities of the manganese compounds and to the present susceptibility measurements on the nickel compound. The table indicates that a transition temperature higher than observed is predicted for the nickel compound from the molecular-field theory in which $T_N = 2zJS(S+1)/3k$. The theory apparently greatly overestimates the value for $NiCl_2 \cdot 4H_2O$, but this is not very disturbing since the molecular-field model is not generally as good as some of the more sophisticated theoretical approaches. Indeed, better agreement may be obtained from the empirical relation of Rushbrooke and Wood,[44]

$$T_C = 5J(z-1)[11S(S+1)-1]/96k\,, \qquad (14)$$

which was obtained for Heisenberg ferromagnets with cubic lattices. Green's-function theories generally predict[45] ferromagnetic and antiferromagnetic transitions to occur at the same temperature, although Rushbrooke and Wood[46] indicate the antiferromagnetic one should be a few percent higher. The predictions for a simple cubic lattice (with $z=6$), using the experimental values for zJ, are shown in Table IV and obviously give better agreement than the molecular-field-theory predictions. The use of Eq. (14) seems justified since it has been pointed out that a simple cubic lattice may well describe the manganese compounds,[5] there being six nearly equivalent near neighbors to a given manganese ion in $MnCl_2 \cdot 4H_2O$.

However, the prediction for $NiCl_2 \cdot 4H_2O$ is still anomalously high and it seems that, at least for the nickel compound, a further consideration of the correctness of the use of $z=6$ must be made. Although the approach used for determining z in Table I cannot be trusted quantitatively, the trend is obvious: $NiCl_2 \cdot 4H_2O$ has a lower magnetic coordination number than either of the manganese isomorphs. In fact, considering the axial character of the Ni^{2+} ion observed in this study and the nearest-neighbor arrangement in the lattice, it does not seem unreasonable to consider a value of 2 for z in $NiCl_2 \cdot 4H_2O$. In that case, $|J/k| = 2.62$° K and the Rushbrooke–Wood calculation predicts $T_C = 2.87$° K. Although this value for J is about 50 times larger than that calculated for $MnCl_2 \cdot 4H_2O$, it still is a reasonable value (it is approximately twice that derived for the compound $NiCl_2 \cdot 6H_2O$[47]) and the large increase over the value for the manganese isomorph apparently reflects the axial nature of the nickel compound. Although the lattice parameters indicate the nearest-neighbor distances may be slightly decreased in $NiCl_2 \cdot 4H_2O$ compared to those in $MnCl_2 \cdot 4H_2O$, the difference would not reasonably be expected to cause a great change in the exchange interactions. It must, however, be pointed out that $z=2$ implies chains which certainly do not exist in $NiCl_2 \cdot 4H_2O$ and that the validity of the Rushbrooke–Wood calculation for $z=2$ may be questioned. An experimental determination of the value of J, independent of z, would be most useful.

A further point of interest is the effect of the crystal field anisotropy on the ordering temperature. (Note that the discussion of the transition temperature up to this point has assumed zero anisotropy.) Theory[45,48–50] predicts that the transition temperature is a function of the anisotropy, $T_N = T_N(D)$, and that it will increase as the ratio D/J increases. Thus the present study provides a useful check on the theoretical predictions. The value of D/J determined for $NiCl_2 \cdot 4H_2O$ in the present work, $11.5/2.62 = 4.41$, has been used in the molecular-field approximation[45] with $z=2$ to predict a value of $T_N(D)/T_N(0) = 1.31$. This value,

TABLE IV. Comparison of the observed transition temperatures of the three isomorphs with the Rushbrooke–Wood predictions for the transition temperatures (for $z=6$, using the observed zJ/k values of Table III).

	$MnCl_2 \cdot 4H_2O$	$MnBr_2 \cdot 4H_2O$	$NiCl_2 \cdot 4H_2O$
Rushbrooke–Wood T_C (°K)	1.41	1.96	4.80
Experimental T_N (°K)	1.62	2.14	2.99

when used in conjunction with the above prediction of $T_C(0) = 2.87$ results in a predicted value of 3.76 °K for $T_N(D)$. Thus the molecular-field approach predicts too high a value for the transition temperature.

Although it might be expected that the predictions of Green's-function approaches[45] would give more reliable estimates, it appears that they do not for the present case. Most of the calculations and results published for those theories have been based on cubic systems, so it would seem (again, on the basis of nearest-neighbor arrangements in $NiCl_2 \cdot 4H_2O$) that the results might be used for this system. (The Green's-function zero-anisotropy predictions, in fact, give results very near to those of the Rushbrooke–Wood predictions in Table IV.) However, the choice of $z = 2$ made above creates an inconsistency in the application of the theoretical results. The Green's-function prediction for a spin-1 simple cubic lattice with $D/J = 4.41$ gives a value for $T_N(D)/T_N(0)$ between 1.4 and 1.5.[45] This is greater than the molecular-field prediction and if the coordination number of 2 is used in the Green's-function calculations the value increases even more.

So it would seem that the molecular-field theory describes the effect of crystal field anisotropy on the transition temperature better than Green's-function approaches do. Clearly, however, the present system is not the most ideal one for checking the validity of the theory. Studies of a system which is cubic would eliminate several of the problems encountered in considering the present data.

ACKNOWLEDGMENTS

The assistance of Dr. E. Tillmanns in the x-ray work is gratefully acknowledged. This research was supported by the National Science Foundation.

[1]S. A. Friedberg and J. D. Wasscher, Physica (Utr.) **19**, 1072 (1953).
[2]W. E. Henry, Phys. Rev. **94**, 1146 (1954).
[3]M. A. Lasheen, J. Van den Broek, and C. J. Gorter, Physica (Utr.) **24**, 1061 (1958).
[4]M. A. Lasheen, J. Van den Broek, and C. J. Gorter, Physica (Utr.) **24**, 1076 (1958).
[5]A. R. Miedema, R. F. Wielinga, and W. J. Huiskamp, Physica (Utr.) **31**, 835 (1965).
[6]G. S. Dixon and J. E. Rives, Phys. Rev. **177**, 871 (1969).
[7]J. E. Rives, Phys. Rev. **162**, 491 (1967).
[8]J. N. McElearney, H. Forstat, and P. T. Bailey, Phys. Rev. **181**, 180 (1969).
[9]R. D. Spence and V. Nagarajan, Phys. Rev. **149**, 191 (1966).
[10]T. A. Reichert, R. A. Butera, and E. J. Schiller, Phys. Rev. B **1**, 4446 (1970).
[11]T. A. Reichert and W. F. Giauque, J. Chem. Phys. **50**, 4205 (1969).
[12]W. F. Giauque, R. A. Fisher, G. E. Brodale, and E. W. Hornung, J. Chem. Phys. **52**, 2901 (1970).
[13]W. F. Giauque, E. W. Hornung, G. E. Brodale, and R. A. Fisher, J. Chem. Phys. **52**, 3936 (1970).
[14]W. F. Giauque, R. A. Fisher, E. W. Hornung, and G. E. Brodale, J. Chem. Phys. **53**, 1474 (1970).
[15]A. Neuhaus, Chem. Erde **5**, 554 (1930).
[16]P. Groth, *Chemishe Kristallographie* (Wilhelm Engleman, Leipzig, 1908), Vol. I.
[17]A. Zalkin, J. D. Forrester, and D. H. Templeton, Inorg. Chem. **3**, 529 (1964).
[18]D. G. Kapadnis and R. Hartmans, Physica (Utr.) **22**, 181 (1956).
[19]Scientific Instruments, Inc., Lake Worth, Fla.
[20]F. G. Brickwedde, H. van Dyk, M. Durieux, J. R. Clement, and J. K. Lagan, J. Res. Natl. Bur. Stand. (U. S.) A **64**, 1 (1960).
[21]N. D. Love, Ph.D. dissertation (Michigan State University, 1967) (unpublished).
[22]Wilbur B. Driver Co., Newark, N. J.
[23]Janis Research Co., Stoneham, Mass.
[24]Cryotronic, Inc., High Bridge, N. J.
[25]W. L. Pillinger, P. S. Jastram, and J. G. Daunt, Rev. Sci. Instrum. **29**, 159 (1958).
[26]A. H. Cooke, in *Progress in Low Temperature Physics*, edited by C. J. Gorter (North-Holland, Amsterdam, 1955), Vol. 1, p. 238.
[27]W. K. Robinson and S. A. Friedberg, Phys. Rev. **117**, 402 (1960).
[28]S. A. Friedberg, Physica (Utr.) **18**, 714 (1952).
[29]M. E. Fisher, Proc. R. Soc. A **254**, 66 (1960).
[30]M. E. Fisher, J. Math. Phys. **4**, 124 (1963).
[31]T. Haseda and M. Date, J. Phys. Soc. Jap. **13**, 175 (1958).
[32]T. Watanabe, J. Phys. Soc. Jap. **17**, 1856 (1962).
[33]B. R. McGarvey, *Transition Metal Chemistry*, edited by R. L. Carlin (Marcel Dekker, New York, 1966), Vol. 3, p. 89.
[34]K. Lonsdale and K. S. Krishnan, Proc. R. Soc. A **156**, 597 (1936).
[35]T. Watanabe, J. Phys. Soc. Jap. **16**, 1131 (1961).
[36]T. Moriya, Phys. Rev. 117, 635 (1970).
[37]J. T. Schriempf and S. A. Friedberg, J. Chem. Phys. **40**, 296 (1964).
[38]R. D. Pierce and S. A. Friedberg, Phys. Rev. B **3**, 934 (1971).
[39]L. G. Polgar and S. A. Friedberg, Phys. Rev. B **4**, 3110 (1971).
[40]A. Herweijer and S. A. Friedberg, Phys. Rev. B **4**, 4009 (1971).
[41]R. B. Flippen and S. A. Friedberg, Phys. Rev. **121**, 1591 (1961).
[42]R. B. Flippen and S. A. Friedberg, J. Appl. Phys. Suppl. **31**, 338S (1960).
[43]T. Haseda and E. Kanda, J. Phys. Soc. Jap. **12**, 1051 (1957).
[44]G. S. Rushbrooke and P. J. Wood, Mol. Phys. **1**, 257 (1958).
[45]J. F. Devlin, Phys. Rev. B **4**, 136 (1971).
[46]G. S. Rushbrooke and P. J. Wood, Mol. Phys. **6**, 410 (1962).
[47]C. Domb and A. R. Miedema, in Ref. 26, Vol. IV, p. 296.
[48]M. E. Lines, Phys. Rev. **156**, 534 (1967).
[49]F. B. Anderson and H. B. Callen, Phys. Rev. **136**, A1068 (1964).
[50]A. Narath, Phys. Rev. **140**, A854 (1965).